UVA irradiation increases ferrous iron release from human skin fibroblast and endothelial cell ferritin: consequences for cell senescence and aging

Matthew J. Smith[1], Mark Fowler[2], Richard J. Naftalin[1*] and Richard C.M. Siow[1]

[1] King's BHF Centre of Research Excellence, School of Cardiovascular Medicine & Sciences, Faculty of Life Sciences & Medicine, 150 Stamford Street, London SE1 9NH, U.K.
[2] Unilever Colworth Science Park, Bedfordshire, U.K.

Short title: UVA irradiation acutely induces Fe (II) loss from cell ferritin

*Correspondence:

Prof Richard J. Naftalin
King's BHF Centre of Research Excellence, School of Cardiovascular Medicine & Sciences, Faculty of Life Sciences & Medicine, 150 Stamford Street, London SE1 9NH, U.K. (email: richard.naftalin@kcl.ac.uk)

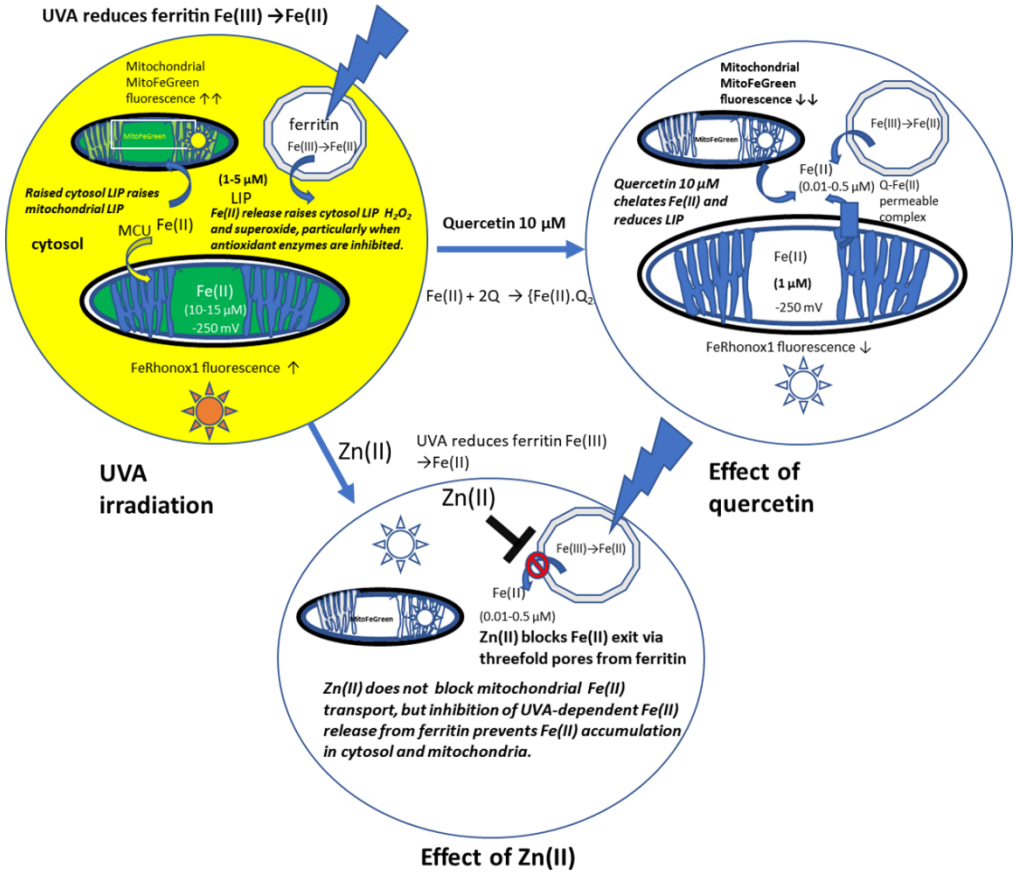

Highlights

- UVA irradiation causes immediate increases in cytosolic and mitochondrial Fe(II) in human dermal fibroblasts and endothelial cells, as monitored by Fe(II) reporters FeRhonox1 and MitoFerroGreen.
- UVA irradiation increases dermal endothelial H_2O_2, monitored using the adenovirus vector Hyper-DAAO-NES.
- UVA-dependent increases in Fe(II) and H_2O_2 are inhibited by $ZnCl_2$ (10 µM) via ferritin's 3-fold iron conducting channels.
- Quercetin reduces UVA dependent Fe(II) signals and H_2O_2 production.
- Inhibition of superoxide dismutase and catalase by tetrathiomolybdate and 3-amino-1, 2, 4-triazole increases and prolongs the cytosolic Fe(II) signal after UVA irradiation.
- UVA-dependent ferritin iron release is the most proximal cause of UV-dependent dermal inflammation.

Abstract

UVA irradiation of human dermal fibroblasts and endothelial cells induces an immediate transient increase in cytosolic Fe(II), as monitored by the fluorescence Fe(II) reporters, FeRhonox1 in cytosol and MitoFerroGreen in mitochondria. Both superoxide dismutase (SOD) inhibition by tetrathiomolybdate (ATM) and catalase inhibition by 3-amino-1, 2, 4-triazole (ATZ) increase and prolong the cytosolic Fe(II) signal after UVA irradiation. SOD inhibition with ATM also increases mitochondrial Fe(II). Thus, mitochondria do not source the UV-dependent increase in cytosolic Fe(II), but instead reflect and amplify raised cytosolic labile Fe(II) concentration. Hence control of cytosolic ferritin iron release is key to preventing UVA-induced inflammation. UVA irradiation also increases dermal endothelial cell H_2O_2, as monitored by the adenovirus vector Hyper-DAAO-NES(HyPer). These UVA-dependent changes in intracellular Fe(II) and H_2O_2 are mirrored by increases in cell superoxide, monitored with the luminescence probe L-012. UV-dependent increases in cytosolic Fe(II), H_2O_2 and L-012 chemiluminescence are prevented by $ZnCl_2$ (10 μM), an effective inhibitor of Fe(II) transport via ferritin's 3-fold channels. Quercetin (10 μM), a potent membrane permeable Fe(II) chelator, abolishes the cytosolic UVA-dependent FeRhonox1, Fe(II) and HyPer, H_2O_2 and increase in MitoFerroGreen Fe(II) signals. The time course of the quercetin-dependent decrease in endothelial H_2O_2 correlates with the decrease in FeRhox1 signal and both signals are fully suppressed by preloading cells with $ZnCl_2$. These results confirm that antioxidant enzyme activity is the key factor in controlling intracellular iron levels, and hence maintenance of cell antioxidant capacity is vitally important in prevention of inflammation initiated by labile iron and UVA.

List of abbreviations: 3-amino-1, 2, 4-triazole (ATZ); dihydroriboflavin 5'-phosphate ($FMNH_2$); Labile iron pool, (LIP); riboflavin nucleotide, FMN; degrees of freedom, d.f.; Desferrioxamine, DFO; Polyethylene glycolated superoxide dismutase, PEG-SOD; photon, hv; normal human dermal fibroblasts, NHDF; superoxide dismutase (SOD); tetrathiomolybdate (ATM) ; HBSS, Hank's buffered saline solution

Introduction

To date the individual roles of subcellular components to cytosolic UVA-dependent iron increase have been difficult to resolve, as temporal and spatial resolutions of iron reporters following changes in labile iron pool have been insufficient [1,2]; e.g. radioactive ^{59}Fe label distribution [3] and turn-off reporters of cytosolic iron such as calcein [4] or PhenGreen-SK [5]. The newly available cytosolic ferrous iron sensitive turn-on fluorescent probes (FeRhonox1) [6] and mitochondrial Fe(II) (MitoFerroGreen) [7] potentially improve both the time resolution and reliability of observed changes in cytosolic and mitochondrial labile iron pool (LIP) following UVA irradiation. Use of these probes allows rapid monitoring of the effects of UVA irradiation on intracellular iron mobilization. This can be readily sourced to ferritin, as iron diffusion through ferritin's shell hydrophilic 3-fold pores is specifically inhibited by Zn(II), which binds with high affinity to sites within the pore [8–11].

The availability of specific mitochondrial Fe(II) reporters [12–16] has shown that labile Fe(II) exists within the mitochondrial space at higher concentrations, around 5-7 μM, than in the cytosol with much higher concentrations reported in Friedrich's ataxia ≈ 15μM) [13]. This high concentration of labile iron results mainly from the large negative mitochondrial membrane potential ≈-250 mV [17]. Thus, mitochondria in Friedrich's ataxia or iron overload are particularly vulnerable to UVA irradiation-induced damage, as corroborated by the observation that mitochondrial iron chelators reduce UV-induced apoptosis [12,13,18]. Although iron is present is substantial amounts in mitochondria, it is unlikely to be present in dermal mitochondrial ferritin [19] unlike its presence in brain, testis [19] and heart [20]. Instead, it is likely to be present in dermal mitochondria and iron-sulphur clusters which are essential components both in heme synthesis and regulation of aconitase [21].

Nevertheless, given the mitochondrial high iron concentration and the large numbers of mitochondria [16], amounting to 20-25% of cell iron [22], it seems likely that they are a source of the increase in cytosolic Fe(II) following UVA-irradiation. Whether mitochondria are a major source of raised dermal cytosolic labile Fe(II) following UVA irradiation remains an unanswered question. Thus, examination of the effect of UVA on the subsequent intramitochondrial Fe(II) generated signal with the MitoFeGreen Fe(II) probe is of considerable interest [7].

Another favoured hypothesis for the source of raised intracellular labile iron following UVA irradiation is that ferritin iron is recycled following lysosomal damage due to excess H_2O_2 and UVA irradiation, [23,24]. These challenges produce similar lytic effects on lysosomes to those from superoxide and hydroxyl radicals generated by cytosolic Fenton reactions and redox cycling [4,25]. Furthermore, release of lysosomal contents leads to mitochondrial damage [26] and can be prevented by the iron chelator desferrioxamine (DFO) [1].

In vitro, H_2O_2 inhibits iron release from ferritin [9,27], because it changes ferritin iron from the reduced ferrous Fe(II) to the oxidized ferric Fe(III) state [8]. However, exogenously sourced H_2O_2 has variable effects on cytosolic labile iron, e.g. in J16 Jurkat cells cytosolic iron is increased but unaffected in HJ16 cells [4]. Increased calcein-chelatable iron and lysosomal destabilization by exogenous H_2O_2 was prevented by DFO [4]. The ratio of extracellular to intracellular H_2O_2 is estimated to be approximately 100:1 [28]. Thus, apparently iron facilitates superoxide and other radical product formation from H_2O_2, e.g. ascorbate free radical and $FMN^{\bullet-}$, as a result of antioxidant enzyme activity and redox cycling reactions [29–31].

Singlet oxygen, $^1O_2$ formed during exposure of dermal photosensitizers to UVA, may be another source of radical formation [32–35]. Similar difficulties have arisen in characterizing the role of H_2O_2 in photochemical activation of oxidative damage to membrane lipids and DNA, since UVA activation is known to result in iron release and subsequent oxidation of membrane lipids [29,36–40].

To elucidate the roles of iron and individual reactive oxygen species in inflammatory processes initiated by UVA irradiation or exogenous H_2O_2, we examined time-dependent changes in intracellular labile iron Fe(II), H_2O_2 and superoxide before and after varying UVA irradiation doses in human dermal fibroblasts and endothelial cells. Additionally, we investigated the effects antioxidant enzymes superoxide dismutase and catalase on UVA-dependent iron mobilization by monitoring the effects of the superoxide dismutase inhibitor, tetrathiomolybdate (ATM)[9,41] and catalase inhibitor aminotriazole (ATZ) [42].

To confirm the role of ferritin in UVA-dependent Fe(II) release, we examined whether Zn (II) blocked the UVA-dependent release of iron into the cytosol and its effects on intracellular H_2O_2 and mitochondrial Fe(II) using the new fluorescence probe FeRhonox1 [6]. Additionally, exogenous H_2O_2 was added to cells to determine its direct effect on intracellular iron and H_2O_2 using reporters of both intracellular Fe(II) and H_2O_2 (**see Methods**). As quercetin has both high membrane permeability and high affinity for Fe(II) [43], both Zn (10 μM) and quercetin (10 μM) were used to reverse the UVA-dependent increase in FeRhonox1, and thereby confirm the efficacy of the switch-on Fe(II) reporters and prevention of Fe(II)-dependent increase in H_2O_2 and superoxide formation.

Methods

Cell culture. Normal human dermal fibroblasts (NHDFs) were cultured in phenol red-free Dulbecco's modified Eagles Medium (DMEM) (Sigma), supplemented with 10% foetal bovine serum (FBS), 4mM L-glutamine (Sigma) and 1% penicillin/streptomycin (Sigma) under standard conditions (37℃, 5% CO_2). Human dermal blood endothelial cells (HDBECs) (PromoCell, Germany) were grown in MV2 basal growth media (PromoCell, Germany) supplemented with 5% FBS, endothelial cell supplement kit (PromoCell, Germany) and 1% penicillin/streptomycin under standard conditions (37℃, 5% CO_2). Cells were cultured in black 96-well

plates for fluorescent plate-reader assays and white 96-well plates (Greiner Bio-One, Austria) for luminescence experiments. Treatments consisted of 4-10 μM $ZnCl_2$, 500U/ml superoxide dismutase-polyethylene glycol (pSOD), catalase-polyethylene glycol (pCAT), 4μM ammonium tetrathiomolybdate (ATM/SODinh) and 2mM 3-amino-1 2 4-triazole (3-ATZ/CATinh) added 30 min prior to experiments.

UVA treatment. Cells were exposed to UVA (365nm) for 1-10 min (approx. 0.8-8 kJ/m^2) using a UVL-56 lamp (UVP) in an incubator under standard conditions (37 ℃, 5% CO_2).

Monitoring cytoplasmic labile iron with a selective Fe(II) probe FeRhoNox1. Measurement of intracellular UV-induced iron release was monitored using FeRhoNox-1, an intracellular fluorescent probe specific for the detection of labile iron Fe(II) [6]. Normal human dermal fibroblasts (NDHFs) were grown to confluence in 96 well plates in DMEM and, when stated, supplemented with 0, 10 or 40μM of zinc ($ZnCl_2$). Cells were incubated with 5μM FeRhoNox1 (Goryo Chemical, Japan) for 1 h prior to assays, before washing twice with PBS followed by addition of Hank's Balanced Saline Solution (HBSS) (Gibco) containing stated treatments and incubated for 20 min before an assay.

Cell in microtiter plates were placed in a CLARIOstar plate-reader (BMG LabTech) which maintains a defined atmosphere (5% CO_2, 37°C). Fluorescent readings (Ex.535nm/Em.569nm) were obtained at 1 min intervals. A baseline reading was established for 20 min before the plate was removed to an incubator of the same atmospheric conditions, and the wells exposed to UVA light (360nm, 0.8-8 kJ/m^2) for 1, 5 or 10 min. The plate was then returned to the plate-reader for further readings.

Monitoring mitochondrial labile iron with a selective mitochondrial Fe(II) probe MitoFerroGreen. MitoFerroGreen is a fluorescent probe specific for the detection of Fe (II) in the mitochondria [7]. Cells were incubated with 5μM MitoFerroGreen (Dojindo, Japan) for 1 h prior to assays, before being washed twice and the addition of HBSS. (Gibco). Where stated, treatments were added to HBSS and cells incubated for 20 min prior to assay. Fluorescent readings (Ex/Em 505/535nm) were taken at 1 min intervals using the CLARIOstar plate reader (BMG Labtech). For UVA treatment, the plate was removed to an incubator of the same atmospheric conditions and the wells exposed to UVA light (360nm) for 1, 5 or 10 min (0.8-8 kJ/m^2). The plate was then returned to the plate-reader for further readings.

Reactive oxygen species generation. Cells were incubated with the chemiluminescent probe L012 (10μM) in HBSS. Chemiluminescence was measured in a CLARIOstar plate reader at 1 min intervals according to methods reported previously [44].

Monitoring intracellular hydrogen peroxide with the molecular probe HyPer using a multiwell plate reader. Cells were transfected with HyPer-DAAO-NES (HyPer) adenovirus vector (D-amino acid oxidase-nuclear export signal) (kindly provided by Professor Thomas Michel, Harvard University) at a multiplicity of infection (MOI) of 300. After 24 h of incubation, cells were washed three times with PBS and grown for a further 48 h before experimentation. Fluorescent readings were taken in HBSS and where stated, treatments were added

to cells then incubated for 20 min prior to assay. HyPer ratiometric fluorescent signals were acquired using the CLARIOstar plate reader (BMG LabTech) at 1 min intervals. These fluorescent signals are reported as a ratio of Ex 490/420 Em 520nm. The advantage of HyPer is that it is a dynamic reversible probe for intracellular H_2O_2 and has many advantages over other fluorescent probes that are generally irreversible and hence unsuited to monitoring dynamic changes in H_2O_2[45,46] .

Results

UVA irradiation increases skin fibroblast cytosolic chelatable iron

Once FeRhonox1 was loaded and the fluorescence output equilibrated, as judged by the output from the Clariostar plate reader, the plate was exposed to UVA for varying times outside the platereader and then replaced immediately. The break in the output reading is shown in **Figure 1A**, which shows a typical readout of FeRhonox1 signals in normal human dermal fibroblasts (NDHF) exposed for 5 min to UVA irradiation (4 kJ/m^2). Immediately after UVA irradiation, there is a sharp increase in the FeRhonox1 fluorescence ($P < 0.001$), that is increased by longer irradiation (not shown). The increase in FeRhonox1 signal is enhanced when the SOD inhibitor ATM is present. Application of $ZnCl_2$ (10 μM) prior to UVA irradiation prevents the UVA-dependent increase in FeRhonox1 signal ($P < 0.001$) (**Figures 1A, 1B**). Zn is effective in inhibiting iron mobilization over a range of UVA irradiation form 1-10 min (0.8-8 kJ/m^2). These findings provide useful confirmation that the most likely source of iron for the UV-dependent increase in cytosolic iron is likely to be cytosolic ferritin. Low concentrations of Zn have been shown to block ascorbate and iron-dependent ferritin iron mobilization in ferritin solutions, [9].

Figure 2A show a typical averaged readout of FeRhonox1 signals plotted as a histogram in fibroblast control cells (prior to UVA irradiation) and after 1 and 5 min UVA irradiation (0.8 and 4 kJ/m^2). The increment in FeRhonox1 signal is enhanced by longer irradiation times. In unirradiated cells, the superoxide dismutase inhibitor, ammonium tetrathiomolybdate (4 μM ATM)[47], decreased the steady state FeRhonox1 signal, as did the catalase inhibitor 3-amino-1, 2, 4-triazole (3-ATZ/CATinh). However, following UVA irradiation, both ATM (**Figure 2B**) and ATZ increased the cellular FeRhonox1 response to UVA irradiation.

The raised increase in FeRhonox1 signal after UVA irradiation, which is mainly dependent upon cell superoxide dismutate inhibition, supports the view that superoxide induces iron mobilization [27,48] and hence increases the labile iron pool. These results indicate that UVA irradiated control skin fibroblasts are normally protected from excessive increases in cytosolic Fe(II) from UVA mobilized iron by the action of antioxidant enzymes superoxide dismutase and catalase, and probably also glutathione peroxidase [49], which separately and together prevent superoxide formation and hence retard superoxide-dependent iron mobilization from ferritin.

The effect of a catalase inhibitor ATZ on the UVA-dependent increment in FeRhonox1 (**Figure 2B**) suggests that UVA-dependent increases in intracellular H_2O_2 also cause an increase in the labile iron pool. This is likely to be due to H_2O_2 formation as a result of superoxide dismutase activity. As already demonstrated in **Figures 1A and 1B**, exposure to low concentrations of $ZnCl_2$ prevents UV-dependent iron release in dermal fibroblasts and endothelial cells, suggesting that the bulk of the increase in cytosolic Fe(II) following UVA irradiation stems from ferritin iron mobilisation.

Effect of UVA irradiation on intracellular H_2O_2 in dermal endothelial cells monitored by HyPer fluorescence

As stated in the Methods, intracellular H_2O_2 was monitored with the aid of adenovirus vector Hyper-DAAO-NES transfection into dermal endothelial cells. Although fibroblasts show a small HyPer response, the signal to noise ratio in these cells is too large to give reliably significant results. As HyPer transfected dermal endothelial cells show significant responses to UVA and exogenous H_2O_2, all subsequent experiments using HyPer were conducted with dermal endothelial cells. Notably, dermal endothelial cells take up more FeRhonox1 than fibroblasts and therefore exhibit a larger response to UVA**.**

Effect of exogenous H_2O_2 on intracellular FeRhonox1 signal in dermal endothelial cells and fibroblasts.

An increased HyPer H_2O_2 signal following addition of exogenous H_2O_2 (100 µM) confirms that the HyPer probe acts as an effective probe for intracellular H_2O_2. However, the effect is relatively short-lived (4-10 min) **(Figure 3A).** The duration of the H_2O_2 transient is prolonged with exposure to higher H_2O_2 concentrations and by inhibition of SOD. Addition of exogenous H_2O_2 (100 µM) to dermal endothelial cells results in a transient increase in FeRhonox1 signal **(Figure 3B)**. These findings support the view that the co-presence of superoxide and H_2O_2 amplify ferritin iron mobilization (not shown in this Figure).

The time course of the decrease from the peak signal closely matches the decrease from peak signal obtained with H_2O_2 in endothelial cells transfected with HyPer **(Figure 3A).** This finding corroborates a recent report [4], showing an increase in labile iron pool following Jurkat cell exposure to varying concentrations of exogenous H_2O_2.

Effects of UVA exposure on cytosolic H_2O_2 in dermal endothelial cells

HyPer responses were monitored in endothelial cells in the absence prior to or after UVA exposure. Averaged signals are shown in **Figure 4A** and after 5 min UVA irradiation the intracellular HyPer signal increases by ≈2-fold ($P < 0.01$) and in the presence of a SOD inhibitor (20 µM ATM) by > 3-fold ($P < 0.001$). This can be compared with the response to exogenous H_2O_2 (100 µM) which increases the HyPer response 2.5-fold ($P< 0.001$). The likely source of this extra superoxide particularly with Fe(II) enriched cytosol is from iron catalysed Fenton reaction [50].

In dermal endothelial cells, as in fibroblasts, similar qualitative effects of the SOD inhibitor ATM are observed for iron release. Thus, it is evident that intrinsic antioxidant SOD activity normally prevents significant net

iron mobilization from ferritin. This finding implies that a major cause of UVA-dependent iron release to the cytosol results from superoxide anion formation, a known source of electrons which reduces ferritin core Fe(III) to soluble, mobile and chelatable Fe(II), [48,51]. In addition to raising dermal endothelial H_2O_2, SOD inhibition by ATM (4 μM) increases the FeRhonox1 signal after 5 min UVA irradiation ($P < 0.001$) **(Figure 3).**

***Effect of quercetin on FeRhonox1 signals and intracellular HyPer* in dermal endothelial cells**

Quercetin (10 μM) was added to the dermal endothelial bathing solution 100 min after UVA exposure, to determine the reversibility of the FeRhonox1 response to raised intracellular Fe(II) and of HyPer to raised H_2O_2. Quercetin at concentrations in excess of labile iron, acts as a very high affinity Fe(II) chelator [43,52,53]. Quercetin reduces both dermal fibroblast and endothelial cell FeRhonox1 signals ($t_{1/2} \approx 7$ min) (**Figure 4B and S1**). The quercetin-dependent decrease in FeRhonox1 signal is significantly larger after exposing the cells to inhibitors of catalase and superoxide dismutase (Supplemental Figures S1B and S1C). This larger decrement in intracellular Fe(II) after quercetin chelation is consistent with the raised intracellular iron concentration, as has already been shown following exposure to antioxidant enzyme inhibitors **(Figures 2B** and **4B).**

Quercetin also rapidly reduces the intracellular HyPer signal observed after UV irradiation of dermal endothelial cells **(Figure 4C).** This finding signifies that iron chelation reduces reactive oxygen species production, and hence the redox cycling of these products with consequent reduction in intracellular H_2O_2 concentration. These latter results all point to a positive correlation between intracellular H_2O_2 and labile iron pool levels and corroborate the findings of Qenaei et al [4]. However, our results with cultured dermal endothelial cells are dissimilar to the observed effects of H_2O_2 on ferritin in solution [9,27]. Addition of H_2O_2 to ferritin solutions strongly inhibits ascorbate-dependent iron mobilization. It is likely that the net effect of either addition of exogenous H_2O_2 or direct generation of intracellular H_2O_2 with raised labile iron, is to catalyse electrons production of electrons that reduce Fe(III) and thereby further increase labile cytosolic Fe(II) by redox cycling of iron and superoxide, H_2O_2 and hydroxyl radicals[54].

Evidence of increased reactive oxygen luminescence following UVA irradiation in dermal fibroblasts

Use of luminescence reporters, such as L-012, provide useful corroboration that UVA enhances intracellular free radical production involving oxygen species (**Supplemental Figure S2**). It is evident that UVA enhances luminescence, although longer irradiation times reduced the signal. It is also apparent, from the luminescence enhancement observed with PEG-catalase and PEG-SOD, that L012 is responding primarily to cytosolic superoxide signals. The significant reduction in luminence with quercetin corroborates previous findings showing that quercetin is an effective quencher of free radicals and Fe(II) chelator [52,55,56].

Effect of UVA irradiation on mitochondrial labile iron in dermal endothelial cells

As already mentioned, mitochondria have a very high iron concentration, amounting to approximately 20-25% of total cell iron [22,57,58]. Thus, mitochondria are a plausible source of the increase in cytosolic Fe(II) following UVA-irradiation. To ascertain whether this is the case, we examined the effects of UVA on mitochondrial Fe(II) using the mitochondrial Fe(II) reporter MitoFerroGreen (see Methods). Following UVA irradiation of dermal endothelial cells, an increase mitochondrial iron is observed. Additionally, intra-mitochondrial labile iron signal is further increased in cells treated with SOD inhibitor ATM (4 μM) (**Figure 5**).

SOD inhibition increases UVA-dependent mitochondrial labile iron increase in dermal fibroblasts

Although both dermal fibroblasts and endothelial cells respond in similar ways to UV with respect to ferritin dependent iron release, we further compared the effects of UVA on mitochondrial labile iron signals in dermal fibroblasts loaded either with FeRhonox1 or MitoFerroGreen to compare UV induced changes in cytosolic and mitochondrial iron in the same cell preparation at the same time.

Normal dermal fibroblasts were treated with PEG-SOD (500U/ml) and SOD inhibitor ATM (4μM), before exposure to UVA for 1, 5 and 10 min (≈0.8-8 kJ/m^2). Labile iron in the mitochondria was measured using the MitoFerroGreen fluorescent probe. As with UVA effects on cytosolic Fe(II) reported by FeRhonox1, when $ZnCl_2$ is applied prior to UVA it prevents the increase in mitochondrial Fe(II) **(Figure 5A)**. Moreover, following addition of quercetin(10 μM), there is a rapid decline in mitochondrial Fe(II), suggesting that mitochondrial iron levels change in parallel with cytosolic iron **(Figure 5B).**

Zinc reduces the basal level of mitochondrial iron

As shown in **Figures 5B** and **Supplemental Figure S3**, treatment of dermal fibroblasts with the SOD inhibitor ATM (4μM) and zinc chloride (40μM) lead to increases in labile iron in the mitochondria. Since there is no evidence of any immediate UVA dependent decrease in mitochondrial Fe(II) signal, evidently the rise is cytosolic Fe(II) following UVA irradiation cannot be sourced from mitochondria.

Discussion

The novel findings in this study are that UVA irradiation of dermal fibroblasts and endothelial cells leads to mobilization of ferritin iron and a subsequent rise in cytosolic Fe(II) and H_2O_2 and mitochondrial Fe(II). These increases are normally masked by intracellular antioxidant enzyme activities, namely superoxide dismutase and catalase, which when inhibited lead to enhanced and prolonged rises in cytosolic and mitochondrial Fe(II) and H_2O_2 and superoxide activities. Much of the variability reported previously in cellular responses to UVA may now be assigned to variable amounts of ferritin iron and variable activities of antioxidant enzymes [4]. Previous work has shown that exposure of dermal fibroblasts to UVA (0-12 J/cm^2) [59,60] results in partial inactivation of antioxidant enzymes catalase and superoxide dismutase, although glutathione

peroxidase and glutathione reductase activities were unaffected. Thus much of the increased sensitivity of aging skin to UV may also be ascribed to variability in these factors [61,62].

The underlying processes of photolytic and ligand induced iron release from ferritin [63,64] are very similar to those well described in other ferrihydrites, such as goethite and magnetite [65–69]. In brief, photoactivation of the surface iron-hydroxo complexes with siderophoric ligands, such as citric or ascorbic acid, leads to charge transfer to the mineral surface Fe (III) to produce Fe (II) and subsequent release of soluble ferrous ion and production of hydroxyl, and superoxide free radicals in a series of cyclic reactions **(see Eq 1-3 and Graphical Abstract).**

Eq 1 $[Fe(III)(OH)^{2+}] + h\vartheta \rightarrow Fe(II) + {}^{\bullet}HO$

Eq 2 $[Fe(III)(citrate)] + h\vartheta \rightarrow Fe(II) + citrate^{2\cdot-}$

Eq 3 $citrate^{2\cdot-} + O_2 \rightarrow$ oxidation products $+ CO_2 + O_2^{\cdot-}$

Thus in oxygenated ferrihydrite solutions, UVA irradiation leads to both hydroxyl and superoxide radical production and in the presence of ascorbate [70] and or citrate [71,72] either long lived ascorbate or shorter-lived citrate radicals. These can transfer electrons to Fe(III) with release of soluble Fe(II) from the metal oxide surface. This applies both to geological ferrihydrites and to the biological ferritin ferrihydrite core.

Fe(III) dissolution is stimulated by an Fe(II) chelator which reduces the local Fe(II) activity and thereby prevents or retards Fe(II) reoxidation at the ferroxidase site and hence greatly accelerates net Fe(II) release to the aqueous environment [73]. It is evident from this model that intracellular photolytic reactions depend largely on the availability of Fe(III) sites at the exposed aqueous interface. Both ferritin and hemosiderin are considered to be the major cytosolic targets, although recent Mossbauer spectroscopy studies suggest that much hemosiderin may be produced as a post-mortem artefact [74,75].

Mitochondria are another possible photolytic target, as they contain relatively high concentrations of labile Fe (II) (15 μM) [13,76,77]. Whether this high concentration of labile iron exists within mitochondria *in vivo* remains a debated question. It seems likely that the Fe(III)/Fe(II) ratio is altered by Fe(II) chelators. Mossbauer spectroscopic studies, which do not depend on chelators to report iron concentrations, suggest that much of the mitochondrial iron exists as low mass Fe(III) complexes that are precursors for Fe/S cluster formation [74,75,78,79]. Thus, UV irradiation could lead to an acute increase in mitochondrial Fe(II) as a result of reduction of Fe(III)/S clusters to Fe(II) and consequent electron leakage from mitochondrial complex II [80]. The finding that Zn exposure prior to UV irradiation reduces mitochondrial Fe(II) **(Figure 5A)** appears to confound this hypothesis. However, there is a small UVA-dependent increase in mitochondrial Fe(II) in zinc treated- dermal endothelial cells which is further enhanced in the presence of the SOD inhibitor ATM

(**Figure 5A**). These latter findings suggest that stored mitochondrial Fe(III) is converted to Fe(II) by raised intramitochondrial superoxide following UV irradiation.

Increased intracellular iron raises the intracellular rates of H_2O_2 production **(Figure S1A),** and conversely reducing cytosolic chelatable iron with quercetin reduces levels of cytosolic H_2O_2. The observed correlations between intracellular H_2O_2, superoxide and Fe(II) **(Figure S1A)** in the same endothelial cell preparation, and between quercetin-dependent changes in FeRhonox1 signal and quercetin-dependent decreases in Hyper, FeRhonox1 and L-012 signals, indicate that there is a positive feedback between production of superoxide and hydroxyl radicals and iron release. The results in **Figure 5** indicate that cytosolic iron rapidly equilibrates between the cytosol and mitochondrial spaces since Zn, which inhibits Fe(II) efflux from ferritin, reduces both cytosolic and mitochondrial Fe(II). Moreover, quercetin, which also rapidly reduces cytosolic Fe(II) activity, also reduces mitochondrial Fe(II).

There are several possible routes of mitochondrial iron uptake; DMT1, a di-metal ion proton cotransporter, present in the outer mitochondrial membrane [81,82] and mitoferrins 1 and 2 present in the inner membrane [15,83]. Additionally, the mitochondrial calcium uniporter (MCU)[84] mediates rapid iron uptake and, most likely, the rapid Fe(II) exit we have observed after exposure of dermal endothelial cell to quercetin **(Figure 5).**

Mitochondria may also accumulate iron as a result of defective iron export. The ABCB7/8 transporters are known to be mitochondrial Fe(II) exporters. Overexpression of ABCB8 transporter protects against ferroptosis [85,86] and impairs cardiomyocyte damage caused by the chemotherapeutic drug doxorubicin a known inhibitor of ABCB8 activity [87–89]. Although, currently whether any dermal cell mitochondrial ABCB type transporters are altered during the aging process it is unknown; nevertheless, it is known that aging in dermal cells results in low level of inflammation [90]. Since dermal inflammation leads to increased hepcidin secretion, which suppresses the iron export transporter ferroportin [91], this could be an explanation for cell iron accumulation in senescent skin.

Senescent skin cells, may be particularly susceptible to photolytic damage, as they accumulate large amounts of ferritin iron, possibly resulting from glutathione depletion, leading to impaired ferroptosis [92–94]. Thus, curtailing excessive iron uptake, with topical applications of quercetin [95] or catechins, which have similarly high iron binding affinity [43] together with zinc salts [61] as illustrated in this study, may help to ameliorate some of the senolytic dermal degeneration. Topical application of polyphenols has frequently been recommended as antiaging in cosmetic preparations and apparently polyphenols seem to have some ameliorative actions *in vivo* [96]. The current study would suggest that much of the UVA dependent skin pathology can be ameliorated by prevention or reduction in exposure to a raised dermal labile iron pool.

Conclusions and clinical perspectives

Identification of ferritin as the key intracellular source of the UVA-dependent iron release is important, as it can be blocked by Zn(II) and reduced by the chelating effects of membrane permeable flavanols, such as quercetin or catechins present in green tea [25,53] and thereby attenuate labile iron accumulation. Additionally, more traditional anti-inflammatory drugs such as dexamethasone, which upregulate neutrophil gelatinase associated lipocalin NGAL and protect against oxidative stress by sequestering siderophores[97], may add to the efficacy of these anti-ageing therapies.

Acknowledgements

This work was supported by Unilever (Dr Richard Siow, Dr Mark Fowler) and Heart Research UK (Ref. No. RG2672, Prof GE Mann). The authors are grateful to Professor Thomas Michel, Harvard University who kindly provided the HyPer-DAAO-NES (HyPer) adenovirus vector. The authors are very grateful to Prof Giovanni E, Mann (School of Cardiovascular Medicine & Sciences, King's College London) for his useful advice, encouragement and support during the preparation of this paper.

Authors Contributions

MJS and RJN designed the experiments, MJS conducted all cell cultures and experimentation, RJN and MJS analysed the data and wrote the text and constructed the figures. MJS, MF, RCMS and RJN discussed and revised the paper.

References

[1] C. Pourzand, R.D. Watkin, J.E. Brown, R.M. Tyrrell, Ultraviolet A radiation induces immediate release of iron in human primary skin fibroblasts: the role of ferritin., Proc. Natl. Acad. Sci. U. S. A. 96 (1999) 6751–6756. doi:10.1073/pnas.96.12.6751.

[2] J.L. Zhong, A. Yiakouvaki, P. Holley, R.M. Tyrrell, C. Pourzand, Susceptibility of skin cells to UVA-induced necrotic cell death reflects the intracellular level of labile iron, J. Invest. Dermatol. 123 (2004) 771–780. doi:10.1111/j.0022-202X.2004.23419.x.

[3] S. Roberts, A. Bomford, Ferritin iron kinetics and protein turnover in K562 cells, J. Biol. Chem. 263 (1988) 19181–19187.

[4] A. Al-Qenaei, A. Yiakouvaki, O. Reelfs, P. Santambrogio, S. Levi, N.D. Hall, R.M. Tyrrell, C. Pourzand, Role of intracellular labile iron, ferritin, and antioxidant defence in resistance of chronically adapted Jurkat T cells to hydrogen peroxide, Free Radic. Biol. Med. 68 (2014) 87–100. doi:10.1016/j.freeradbiomed.2013.12.006.

[5] T. Hirayama, H. Tsuboi, M. Niwa, A. Miki, S. Kadota, Y. Ikeshita, K. Okuda, H. Nagasawa, A universal fluorogenic switch for Fe(II) ion based on N-oxide chemistry permits the visualization of intracellular redox equilibrium shift towards labile iron in hypoxic tumor cells, Chem. Sci. 8 (2017) 4858–4866. doi:10.1039/C6SC05457A.

[6] T. Mukaide, Y. Hattori, N. Misawa, S. Funahashi, L. Jiang, T. Hirayama, H. Nagasawa, S. Toyokuni, Histological detection of catalytic ferrous iron with the selective turn-on fluorescent probe RhoNox-1 in a Fenton reaction-based rat renal carcinogenesis model, Free Radic. Res. 48 (2014) 990–995. doi:10.3109/10715762.2014.898844.

[7] T. Hirayama, A. Miki, H. Nagasawa, Organelle-specific analysis of labile Fe(ii) during ferroptosis by using a cocktail of various colour organelle-targeted fluorescent probes, Metallomics. 11 (2019) 111–117. doi:10.1039/c8mt00212f.

[8] X. Yang, P. Arosio, N.D. Chasteen, Molecular diffusion into ferritin: pathways, temperature dependence, incubation time, and concentration effects., Biophys. J. 78 (2000) 2049–2059. doi:10.1016/S0006-3495(00)76752-X.

[9] C. Badu-Boateng, S. Pardalaki, C. Wolf, S. Lajnef, F. Peyrot, R.J. Naftalin, Labile Iron Potentiates Ascorbate-Dependent Reduction and Mobilization of Ferritin iron, Free Radic. Biol. Med. 108 (2017) 94–109. doi:10.1016/j.freeradbiomed.2017.03.015.

[10] K. Zeth, Dps biomineralizing proteins: multifunctional architects of nature., Biochem. J. 445 (2012) 297–311. doi:10.1042/BJ20120514.

[11] G. Zhao, F. Bou-Abdallah, P. Arosio, S. Levi, C. Janus-Chandler, N.D. Chasteen, Multiple pathways for mineral core formation in mammalian apoferritin. The role of hydrogen peroxide., Biochemistry. 42 (2003) 3142–50. doi:10.1021/bi027357v.

[12] O. Reelfs, V. Abbate, R.C. Hider, C. Pourzand, A Powerful Mitochondria-Targeted Iron Chelator Affords High Photoprotection against Solar Ultraviolet A Radiation, J. Invest. Dermatol. 136 (2016) 1692–1700. doi:10.1016/j.jid.2016.03.041.

[13] O. Reelfs, V. Abbate, A. Cilibrizzi, M.A. Pook, R.C. Hider, C. Pourzand, The role of mitochondrial labile iron in Friedreich's ataxia skin fibroblasts sensitivity to ultraviolet A, Metallomics. 11 (2019) 656–665. doi:10.1039/c8mt00257f.

[14] Y. Ma, V. Abbate, R.C. Hider, Iron-sensitive fluorescent probes: Monitoring intracellular iron pools, Metallomics. 7 (2015) 212–222. doi:10.1039/c4mt00214h.

[15] H. Lv, P. Shang, The significance, trafficking and determination of labile iron in cytosol, mitochondria and lysosomes, Metallomics. 10 (2018) 899–916. doi:10.1039/c8mt00048d.

[16] F. Petrat, H. De Groot, U. Rauen, Subcellular distribution of chelatable iron: A laser scanning microscopic study in isolated hepatocytes and liver endothelial cells, Biochem. J. 356 (2001) 61–69. doi:10.1042/0264-6021:3560061.

[17] M. Niwa, T. Hirayama, I. Oomoto, D.O. Wang, H. Nagasawa, Fe(II) Ion Release during Endocytotic Uptake of Iron Visualized by a Membrane-Anchoring Fe(II) Fluorescent Probe, ACS Chem. Biol. (2018) acschembio.7b00939. doi:10.1021/acschembio.7b00939.

[18] C.K. Lim, D.S. Kalinowski, D.R. Richardson, Protection against hydrogen peroxide-mediated cytotoxicity in Friedreich's ataxia fibroblasts using novel iron chelators of the 2-pyridylcarboxaldehyde isonicotinoyl hydrazone class, Mol. Pharmacol. 74 (2008) 225–235. doi:10.1124/mol.108.046847.

[19] H. Yang, M. Yang, H. Guan, Z. Liu, S. Zhao, S. Takeuchi, D. Yanagisawa, I. Tooyama, Mitochondrial ferritin in neurodegenerative diseases, Neurosci. Res. 77 (2013) 1–7. doi:10.1016/j.neures.2013.07.005.

[20] X. Li, P. Wang, Q. Wu, L. Xie, Y. Cui, H. Li, P. Yu, Y.Z. Chang, The construction and

characterization of mitochondrial ferritin overexpressing mice, Int. J. Mol. Sci. 18 (2017). doi:10.3390/ijms18071518.

[21] T.A. Rouault, N. Maio, Biogenesis and Functions of Mammalian Iron-Sulfur Proteins in the Regulation of Iron Homeostasis and Pivotal Metabolic Pathways, J. Biol. Chem. 292 (2017) jbc.R117.789537. doi:10.1074/jbc.R117.789537.

[22] V.S. Richmond, M. Worwood, A. Jacobs, The Iron Content of Intestinal Epithelial Cells and Its Subcellular Distribution: Studies on Normal, Iron-Overloaded and Iron-Deficient Rats, Br. J. Haematol. 23 (1972) 605–614. doi:10.1111/j.1365-2141.1972.tb07095.x.

[23] D.C. Radisky, J. Kaplan, Iron in cytosolic ferritin can be recycled through lysosomal degradation in human fibroblasts., Biochem. J. 336 (Pt 1 (1998) 201–5. http://www.pubmedcentral.nih.gov/articlerender.fcgi?artid=1219858&tool=pmcentrez&rendertype=abstract.

[24] K. Ollinger, U.L.F.T. Brunk, Cellular injury Induced by oxidative stress is mediated through lysosomal damage., Free Radic. Biol. Med. 19 (1995) 565–574.

[25] S. Basu-Modak, D. Ali, M. Gordon, T. Polte, A. Yiakouvaki, C. Pourzand, C. Rice-Evans, R.M. Tyrrell, Suppression of UVA-mediated release of labile iron by epicatechin-A link to lysosomal protection, Free Radic. Biol. Med. 41 (2006) 1197–1204. doi:10.1016/j.freeradbiomed.2006.06.008.

[26] M. Tenopoulou, P.-T. Doulias, A. Barbouti, U. Brunk, D. Galaris, Role of compartmentalized redox-active iron in hydrogen peroxide-induced DNA damage and apoptosis., Biochem. J. 387 (2005) 703–710. doi:10.1042/BJ20041650.

[27] R.F. Boyer, C.J. McCleary, Superoxide ion as a primary reductant in ascorbate-mediated ferritin iron release., Free Radic. Biol. Med. 3 (1987) 389–95. http://www.ncbi.nlm.nih.gov/pubmed/2828195.

[28] H. Sies, Hydrogen peroxide as a central redox signaling molecule in physiological oxidative stress: Oxidative eustress, Redox Biol. 11 (2017) 613–619. doi:10.1016/j.redox.2016.12.035.

[29] P. Morlière, A. Moysan, R. Santus, G. Hüppe, J.C. Mazière, L. Dubertret, UVA-induced lipid peroxidation in cultured human fibroblasts, Biochim. Biophys. Acta (BBA)/Lipids Lipid Metab. 1084 (1991) 261–268. doi:10.1016/0005-2760(91)90068-S.

[30] A. Moysan, I. Marquis, F. Gaboriau, R. Santus, L. Dubertret, P. Morlière, Ultraviolet A – Induced Lipid Peroxidation and Antioxidant Defense Systems in Cultured Human Skin Fibroblasts, J. Invest. Dermatol. 100 (1993) 692–698. doi:10.1111/1523-1747.ep12472352.

[31] F. Funk, J.P. Lenders, R.R. Crichton, W. Schneider, Reductive mobilisation of ferritin iron., Eur. J. Biochem. 152 (1985) 167–72. http://www.ncbi.nlm.nih.gov/pubmed/4043077.

[32] J.L. Liu, Q. Xue, C.G. Liu, F.W. Bai, S. Wada, J.Y. Wang, Chemiluminescence imaging of UVA induced reactive oxygen species in mouse skin using L-012 as a probe, Free Radic. Res. 52 (2018) 1424–1431. doi:10.1080/10715762.2018.1500019.

[33] M. Berneburg, S. Grether-Beck, V. Kürten, T. Ruzicka, K. Briviba, H. Sies, J. Krutmann, Singlet oxygen mediates the UVA-induced generation of the photoaging- associated mitochondrial common deletion, J. Biol. Chem. 274 (1999) 15345–15349. doi:10.1074/jbc.274.22.15345.

[34] K. Jomova, M. Valko, Advances in metal-induced oxidative stress and human disease., Toxicology. 283 (2011) 65–87. http://www.ncbi.nlm.nih.gov/pubmed/21414382 (accessed July 17, 2012).

[35] Z. Yang, J. Qian, A. Yu, B. Pan, Singlet oxygen mediated iron-based Fenton-like catalysis under nanoconfinement, Proc. Natl. Acad. Sci. U. S. A. 116 (2019) 6659–6664. doi:10.1073/pnas.1819382116.

[36] K. Punnonen, C.T. Jansen, A. Puntala, M. Ahotupa, Effects of in vitro UVA irradiation and PUVA treatment on Membrane Fatty Acidds and activities of Antioxidant Enzymes in Human Keratinocytes, J. Invest. Dermatol. 96 (1991) 255–259.

[37] G.F. Vile, R.M. Tyrrell, Uva radiation-induced oxidative damage to lipids and proteins in vitro and in human skin fibroblasts is dependent on iron and singlet oxygen, Free Radic. Biol. Med. 18 (1995) 721–730. doi:10.1016/0891-5849(94)00192-M.

[38] M.J. Burkitt, B.C. Gilbert, Model studies of the iron-catalysed Haber-Weiss cycle and the ascorbate-driven Fenton reaction., Free Radic. Res. Commun. 10 (1990) 265–80. http://www.ncbi.nlm.nih.gov/pubmed/1963164.

[39] N.R. Perron, J.L. Brumaghim, A review of the antioxidant mechanisms of polyphenol compounds related to iron binding., Cell Biochem. Biophys. 53 (2009) 75–100. doi:10.1007/s12013-009-9043-x.

[40] G.R. Buettner, The Pecking Order of Free Radicals and Antioxidants: Lipid Peroxidation, a-Tocopherol, and Ascorbate, Arch. Biochem. Biophys. 300 (1993) 535–543. doi:10.1006/abbi.1993.1074.

[41] J.C. Juarez, M. Manuia, M.E. Burnett, O. Betancourt, B. Boivin, D.E. Shaw, N.K. Tonks, A.P. Mazar, F. Doñate, Superoxide dismutase 1 (SOD1) is essential for H2O2-mediated oxidation and inactivation of phosphatases in growth factor signaling., Proc. Natl. Acad. Sci. U. S. A. 105 (2008) 7147–52. doi:10.1073/pnas.0709451105.

[42] P.L. Merle, C. Sabourault, S. Richier, D. Allemand, P. Furla, Catalase characterization and implication in bleaching of a symbiotic sea anemone, Free Radic. Biol. Med. 42 (2007) 236–246. doi:10.1016/j.freeradbiomed.2006.10.038.

[43] E. Vlachodimitropoulou, P.A. Sharp, R.J. Naftalin, Quercetin-iron chelates are transported via Glucose (GLUT) transporters ., Free Radic. Biol. Med. 50 (2011) 934–44. doi:10.1016/j.freeradbiomed.2011.01.005.

[44] M. He, M. Nitti, S. Piras, A.L. Furfaro, N. Traverso, M.A. Pronzato, G.E. Mann, Heme oxygenase-1-derived bilirubin protects endothelial cells against high glucose-induced damage, Free Radic. Biol. Med. 89 (2015) 91–98. doi:10.1016/j.freeradbiomed.2015.07.151.

[45] V. V. Belousov, A.F. Fradkov, K.A. Lukyanov, D.B. Staroverov, K.S. Shakhbazov, A. V. Terskikh, S. Lukyanov, Genetically encoded fluorescent indicator for intracellular hydrogen peroxide, Nat. Methods. 3 (2006) 281–286. doi:10.1038/nmeth866.

[46] A. Hernández-Barrera, C. Quinto, E.A. Johnson, H.M. Wu, A.Y. Cheung, L. Cárdenas, Using hyper as a molecular probe to visualize hydrogen peroxide in living plant cells: A method with virtually unlimited potential in plant biology, Methods Enzymol. 527 (2013) 275–290. doi:10.1016/B978-0-12-405882-8.00015-5.

[47] S. Choi, S. Park, G.H. Liang, J.A. Kim, Cellular Physiology and Biochemistr y Biochemistry Superoxide Generated by Lysophosphatidyl- choline Induces Endothelial Nitric Oxide Synthase Downregulation in Human Endothelial Cells, Cell Physiol. Biochem. 25 (2010) 233–240.

[48] P. Biemond, H. Van Eijk, A. Swaak, J. Koster, Iron Mobilization from Ferritin by Superoxide Derived from Stimulated polymorphonuclear Leucocytes., J Clin Invest. 73 (1984) 1576–1579.

[49] C. Michiels, O. Toussaint, J. Remacle, Importance of SE-Glutathione peroxidase, catalase, and

Cu/Zn-SOD for cell survival against oxidative stress., Science (80-.). 17 (1994) 235–248.

[50] G. Minotti, S.D. Aust, An investigation into thee mechanism of citrate-FE2+-dependent lipid peroxidation, Free Radic. Biol. Med. 3 (1987) 379–387. doi:10.1016/0891-5849(87)90016-5.

[51] C. Badu-Boateng, R.J. Naftalin, Ascorbate and ferritin interactions: Consequences for iron release in vitro and in vivo and implications for inflammation, Free Radic. Biol. Med. (2018). doi:10.1016/j.freeradbiomed.2018.09.041.

[52] M. Melidou, K. Riganakos, D. Galaris, Protection against nuclear DNA damage offered by flavonoids in cells exposed to hydrogen peroxide: the role of iron chelation., Free Radic. Biol. Med. 39 (2005) 1591–600. doi:10.1016/j.freeradbiomed.2005.08.009.

[53] M. Guo, C. Perez, Y. Wei, E. Rapoza, G. Su, F. Bou-Abdallah, N.D. Chasteen, Iron-binding properties of plant phenolics and cranberry's bio-effects., Dalton Trans. (2007) 4951–61. http://www.pubmedcentral.nih.gov/articlerender.fcgi?artid=2645657&tool=pmcentrez&rendertype=abstract (accessed June 10, 2011).

[54] K. Jomova, S. Baros, M. Valko, Redox active metal-induced oxidative stress in biological systems, Transit. Met. Chem. 37 (2012) 127–134. doi:10.1007/s11243-012-9583-6.

[55] P. Filipe, J.N. Silva, J. Haigle, J.P. Freitas, A. Fernandes, R. Santus, P. Morlière, Contrasting action of flavonoids on phototoxic effects induced in human skin fibroblasts by UVA alone or UVA plus cyamemazine, a phototoxic neuroleptic., Photochem. Photobiol. Sci. 4 (2005) 420–428. doi:10.1039/b416811a.

[56] B.R. Zhou, H. Bin Yin, Y. Xu, D. Wu, Z.H. Zhang, Zhi-Qiang Yin, F. Permatasari, D. Luo, Baicalin protects human skin fi broblasts from ultraviolet A radiation-induced oxidative damage and apoptosis, Free Radic. Res. 46 (2012) 1458–1471. doi:10.3109/10715762.2012.726355.

[57] N.D. Jhurry, M. Chakrabarti, S.P. McCormick, G.P. Holmes-Hampton, P.A. Lindahl, Biophysical investigation of the ironome of human Jurkat cells and mitochondria, Biochemistry. 51 (2012) 5276–5284. doi:10.1021/bi300382d.

[58] B.T. Paul, D. Manz, F. Torti, S. V. Torti, Mitochondria and Iron: Current Questions Bibbin, Expert Rev. Hematol. 10 (2016) 95–118. doi:10.1080/17474086.2016.1268047.Mitochondria.

[59] Y. Shindo, T. Hashimoto, Time course of changes in antioxidant enzymes in human skin fibroblasts after UVA irradiation, J. Dermatol. Sci. 14 (1997) 225–232. doi:10.1016/S0923-

1811(96)00578-6.

[60] S.R. Pinnell, Cutaneous photodamage, oxidative stress, and topical antioxidant protection, J. Am. Acad. Dermatol. 48 (2003) 1–22. doi:10.1067/mjd.2003.16.

[61] A. Kammeyer, R.M. Luiten, Oxidation events and skin aging, Ageing Res. Rev. 21 (2015) 16–29. doi:10.1016/j.arr.2015.01.001.

[62] A. Aroun, J.L. Zhong, R.M. Tyrrell, C. Pourzand, Iron, oxidative stress and the example of solar ultraviolet A radiation, Photochem. Photobiol. Sci. 11 (2012) 118–134. doi:10.1039/c1pp05204g.

[63] J.P. Laulhère, A.M. Labouré, J.F. Briat, Photoreduction and incorporation of iron into ferritins., Biochem. J. 269 (1990) 79–84.

[64] J.S. Rohrer, M. Joo, E. Dartyge, D.E. Sayers, A. Fontaine, E.C. Theil, Stabilization of Iron in a Ferrous form by ferritin., J Biol Chem. 262 (1987) 13385–13387.

[65] Y. Zhu, R. Zhu, L. Yan, H. Fu, Y. Xi, H. Zhou, G. Zhu, J. Zhu, H. He, Visible-light Ag/AgBr/ferrihydrite catalyst with enhanced heterogeneous photo-Fenton reactivity via electron transfer from Ag/AgBr to ferrihydrite, Appl. Catal. B Environ. 239 (2018) 280–289. doi:10.1016/j.apcatb.2018.08.025.

[66] Z. Wang, W.D.C. Schenkeveld, S.M. Kraemer, D.E. Giammar, Synergistic Effect of Reductive and Ligand-Promoted Dissolution of Goethite, Environ. Sci. Technol. 49 (2015) 7236–7244. doi:10.1021/acs.est.5b01191.

[67] Z. Wang, H. Fu, L. Zhang, W. Song, J. Chen, Ligand-Promoted Photoreductive Dissolution of Goethite by Atmospheric Low-Molecular Dicarboxylates, J. Phys. Chem. A. 121 (2017) 1647–1656. doi:10.1021/acs.jpca.6b09160.

[68] P.M. Borer, B. Sulzberger, P. Reichard, S.M. Kraemer, Effect of siderophores on the light-induced dissolution of colloidal iron(III) (hydr)oxides, Mar. Chem. 93 (2005) 179–193. doi:10.1016/j.marchem.2004.08.006.

[69] P. Avetta, A. Pensato, M. Minella, M. Malandrino, V. Maurino, C. Minero, K. Hanna, D. Vione, Activation of persulfate by irradiated magnetite: Implications for the degradation of phenol under heterogeneous photo-fenton-like conditions, Environ. Sci. Technol. 49 (2015) 1043–1050. doi:10.1021/es503741d.

[70] J. Du, J.J. Cullen, G.R. Buettner, Ascorbic acid: Chemistry, biology and the treatment of cancer., Biochim. Biophys. Acta. 1826 (2012) 443–57. http://www.ncbi.nlm.nih.gov/pubmed/22728050 (accessed November 3, 2012).

[71] J. Van der Zee, K.B. BH, C.F. Chignell, T.M.A.R. Dubbelman, J. Van Steveninck, Hydroxyl radical generation by a light-dependent Fenton Reaction, Free Radic. Biol. Med. 14 (1993) 105–113.

[72] M. Oszajca, M. Brindell, Ł. Orzeł, J.M. Dąbrowski, K. Śpiewak, P. Łabuz, M. Pacia, A. Stochel-Gaudyn, W. Macyk, R. van Eldik, G. Stochel, Mechanistic studies on versatile metal-assisted hydrogen peroxide activation processes for biomedical and environmental incentives, Coord. Chem. Rev. 327–328 (2016) 143–165. doi:10.1016/j.ccr.2016.05.013.

[73] J.P. Laulhère, F. Barcelò, M. Fontecave, Dynamic equilibria in iron uptake and release by ferritin., Biometals. 9 (1996) 303–9. http://www.ncbi.nlm.nih.gov/pubmed/8696080.

[74] S.P. McCormick, M.J. Moore, P.A. Lindahl, Detection of Labile Low-Molecular-Mass Transition Metal Complexes in Mitochondria, Biochemistry. 54 (2015) 3442–3453. doi:10.1021/bi5015437.

[75] J.D. Wofford, M. Chakrabarti, P.A. Lindahl, Mössbauer spectra of mouse hearts reveal age-dependent changes in mitochondrial and ferritin iron levels, J. Biol. Chem. 292 (2017) 5546–5554. doi:10.1074/jbc.M117.777201.

[76] F. Petrat, S. Paluch, E. Dogruöz, P. Dörfler, M. Kirsch, H.-G. Korth, R. Sustmann, H. de Groot, Reduction of Fe(III) ions complexed to physiological ligands by lipoyl dehydrogenase and other flavoenzymes in vitro: implications for an enzymatic reduction of Fe(III) ions of the labile iron pool., J. Biol. Chem. 278 (2003) 46403–13. doi:10.1074/jbc.M305291200.

[77] Z.I. Cabantchik, Labile iron in cells and body fluids: Physiology, pathology, and pharmacology, Front. Pharmacol. 5 MAR (2014) 1–11. doi:10.3389/fphar.2014.00045.

[78] T.A. Rouault, Iron-sulfur proteins hiding in plain sight, Nat. Chem. Biol. 11 (2015) 442–445. doi:10.1038/nchembio.1843.

[79] R. Garcia-Serres, M. Clémancey, J.M. Latour, G. Blondin, Contribution of Mössbauer spectroscopy to the investigation of Fe/S biogenesis, J. Biol. Inorg. Chem. 23 (2018) 635–644. doi:10.1007/s00775-018-1534-z.

[80] A. Anderson, A. Bowman, S.J. Boulton, P. Manning, M.A. Birch-Machin, A role for human

mitochondrial complex II in the production of reactive oxygen species in human skin, Redox Biol. 2 (2014) 1016–1022. doi:10.1016/j.redox.2014.08.005.

[81] N.A. Wolff, M.D. Garrick, L. Zhao, L.M. Garrick, A.J. Ghio, F. Thévenod, A role for divalent metal transporter (DMT1) in mitochondrial uptake of iron and manganese, Sci. Rep. 8 (2018) 1–12. doi:10.1038/s41598-017-18584-4.

[82] I. Yanatori, Y. Yasui, M. Tabuchi, F. Kishi, Chaperone protein involved in transmembrane transport of iron, Biochem. J. 462 (2014) 25–37. doi:10.1042/BJ20140225.

[83] L.R. Devireddy, D.O. Hart, D.H. Goetz, M.R. Green, A Mammalian Siderophore Synthesized by an Enzyme with a Bacterial Homolog Involved in Enterobactin Production, Cell. 141 (2010) 1006–1017. http://dx.doi.org/10.1016/j.cell.2010.04.040.

[84] X. Zhang, J.J. Lemasters, Translocation of iron from lysosomes to mitochondria during ischemia predisposes to injury after reperfusion in rat hepatocytes, Free Radic. Biol. Med. 63 (2013) 243–253. doi:10.1016/j.freeradbiomed.2013.05.004.

[85] H. Chang, R. Wu, M. Shang, T. Sato, C. Chen, J.S. Shapiro, T. Liu, A. Thakur, K.T. Sawicki, S.V. Prasad, H. Ardehali, Reduction in mitochondrial iron alleviates cardiac damage during injury, EMBO Mol. Med. 8 (2016) 247–267. doi:10.15252/emmm.201505748.

[86] V. Kumar, A.K. A., R. Sanawar, A. Jaleel, T.R. Santhosh Kumar, C.C. Kartha, Chronic Pressure Overload Results in Deficiency of Mitochondrial Membrane Transporter ABCB7 Which Contributes to Iron Overload, Mitochondrial Dysfunction, Metabolic Shift and Worsens Cardiac Function, Sci. Rep. 9 (2019) 1–16. doi:10.1038/s41598-019-49666-0.

[87] E. Cocco, V. Porrini, M. Derosas, V. Nardi, G. Biasiotto, F. Maccarinelli, I. Zanella, Protective effect of mitochondrial ferritin on cytosolic iron dysregulation induced by doxorubicin in HeLa cells., Mol. Biol. Rep. (2013). doi:10.1007/s11033-013-2792-z.

[88] R. Gordan, S. Wongjaikam, J.K. Gwathmey, N. Chattipakorn, S.C. Chattipakorn, L.H. Xie, Involvement of cytosolic and mitochondrial iron in iron overload cardiomyopathy: an update, Heart Fail. Rev. 23 (2018) 801–816. doi:10.1007/s10741-018-9700-5.

[89] Y. Ichikawa, M. Ghanefar, M. Bayeva, R. Wu, A. Khechaduri, S. V. Naga Prasad, R.K. Mutharasan, T. Jairaj Naik, H. Ardehali, Cardiotoxicity of doxorubicin is mediated through mitochondrial iron accumulation, J. Clin. Invest. 124 (2014) 617–630. doi:10.1172/JCI72931.

[90] J.A. Wright, T. Richards, S.K.S. Srai, The role of iron in the skin and cutaneous wound healing, Front. Pharmacol. 5 JUL (2014) 1–8. doi:10.3389/fphar.2014.00156.

[91] E. Nemeth, Hepcidin Regulates Cellular Iron Efflux by Binding to Ferroportin and Inducing Its Internalization, Science (80-.). 306 (2004) 2090–2093. doi:10.1126/science.1104742.

[92] S. Masaldan, S.A.S. Clatworthy, C. Gamell, P.M. Meggyesy, A.T. Rigopoulos, S. Haupt, Y. Haupt, D. Denoyer, P.A. Adlard, A.I. Bush, M.A. Cater, Iron accumulation in senescent cells is coupled with impaired ferritinophagy and inhibition of ferroptosis, Redox Biol. 14 (2018) 100–115. doi:10.1016/j.redox.2017.08.015.

[93] S. Masaldan, A.I. Bush, D. Devos, A.S. Rolland, C. Moreau, Striking while the iron is hot: Iron metabolism and ferroptosis in neurodegeneration, Free Radic. Biol. Med. (2019). doi:10.1016/j.freeradbiomed.2018.09.033.

[94] Y. Sun, Y. Zheng, C. Wang, Y. Liu, Glutathione depletion induces ferroptosis, autophagy, and premature cell senescence in retinal pigment epithelial cells article, Cell Death Dis. 9 (2018). doi:10.1038/s41419-018-0794-4.

[95] S.R. Kim, K. Jiang, M. Ogrodnik, X. Chen, X.-Y. Zhu, H. Lohmeier, L. Ahmed, H. Tang, T. Tchkonia, L.J. Hickson, J.L. Kirkland, L.O. Lerman, Increased renal cellular senescence in murine high-fat diet: effect of the senolytic drug quercetin, Transl. Res. (2019) 1–12. doi:10.1016/j.trsl.2019.07.005.

[96] O. V. Zillich, U. Schweiggert-Weisz, P. Eisner, M. Kerscher, Polyphenols as active ingredients for cosmetic products, Int. J. Cosmet. Sci. 37 (2015) 455–464. doi:10.1111/ics.12218.

[97] S. Chakraborty, S. Kaur, S. Guha, S.K. Batra, The multifaceted roles of neutrophil gelatinase associated lipocalin (NGAL) in inflammation and cancer, Biochim. Biophys. Acta - Rev. Cancer. 1826 (2012) 129–169. doi:10.1016/j.bbcan.2012.03.008.

Figures and Figure Legends:

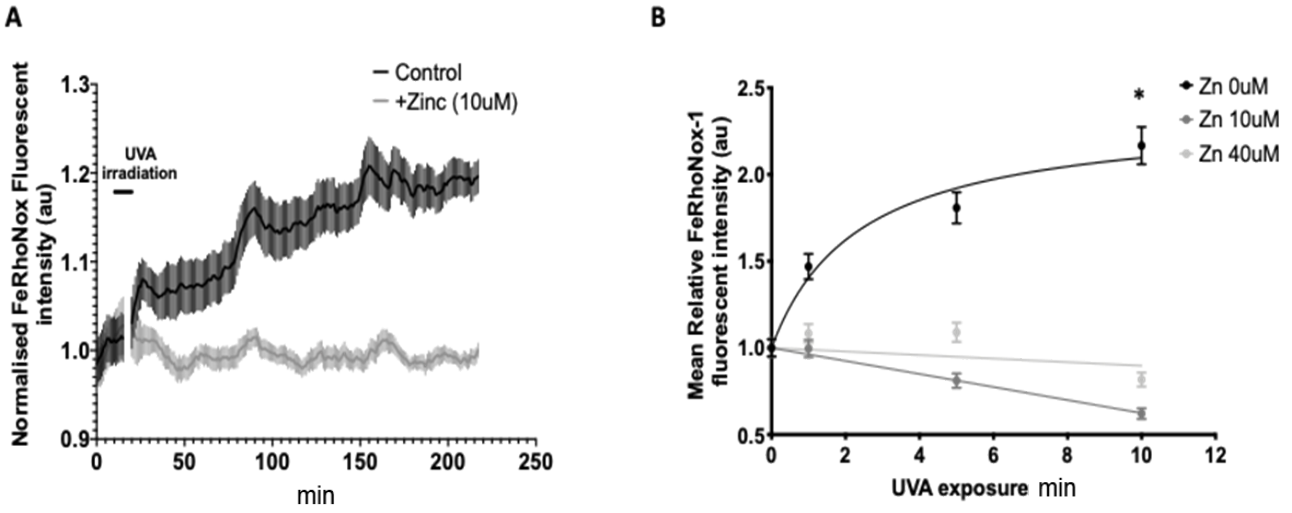

Figure 1. Zinc protects against UVA-induced intracellular iron release in human dermal fibroblasts. (A) Normal human dermal fibroblasts (NHDF) were pre-treated with the SOD inhibitor ATM (4μM) with/without zinc (40μM) and then exposed to UVA irradiation (≈8 kJ/m^2) for 5 min at the indicated time point. Increases in labile iron were measured using the FeRhoNox fluorescent probe. (**B**) Relative FeRhoNox-1 fluorescent intensity in NHDF after UVA exposure (≈0.8-8 kJ/m^2) for 1-10 min following pre-incubation with 0, 10 or 40μM zinc. Fluorescence was measured in a CLARIOStar plate reader. Data denote mean ± SEM, n=3 independent cell cultures, *P < 0.001 vs control.

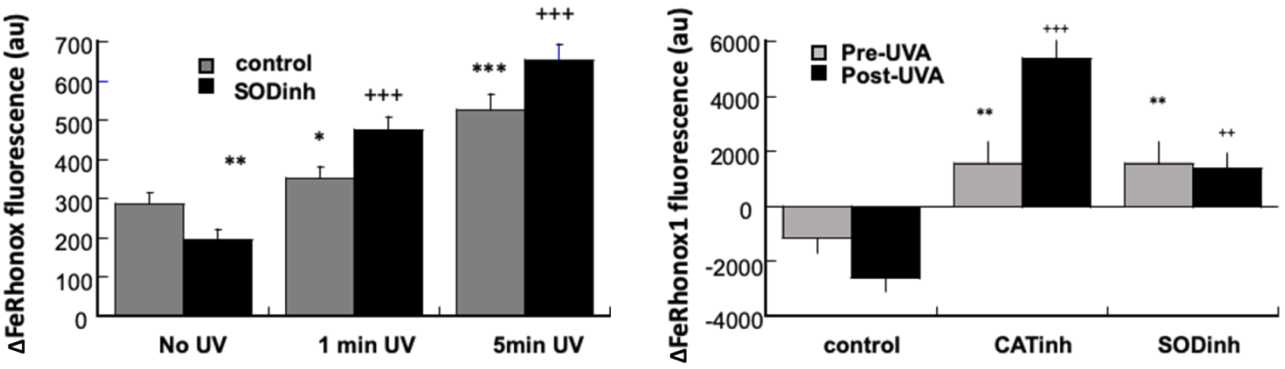

Figure 2. SOD and catalase inhibition increases UVA-dependent labile iron increase in dermal fibroblasts. (**A**) NHDFs were pre-treated with SOD inhibitor ATM (4µM), exposed to UVA for 1 and 5 min (≈0.8 and 4 kJ/m^2) and labile iron measured using the FeRhoNox1 fluorescent probe (after UV versus before UVA: * P<0.05, **P<0.01, ***P<0.001), (after UVA versus before UVA with SOD inhibitor ++ P < 0.01 and ++ P<0.001).

(**B**) NHDFs were irradiated for 5 min with UVA (4 kJ/m^2) and the mean difference in FeRhoNox1 signal measured. Pre UVA (grey bar) difference between signal at (20 min - 40 min) and black bar difference between after 5 min UVA irradiation (60 min - 80 min) *(see time course in Figure 1A)* treated with 2mM Catalase inhibitor 3-ATZ (CATinh) or SOD inhibitor ATM (4µM). Data denote means ± S.E.D n=3 independent wells,Difference between inhibited enzyme condition and control before UV (grey bars) **P<0.01 and differences between enzyme inhibitions after UVA irradiation anc control after UVA irradiation (black columns(++P < 0.01 and +++ P<0.001). Thus both catalase and SOD inhibition significantly increase the FeRohnox1 signals before UVA irradiation and after UVA irradiation.

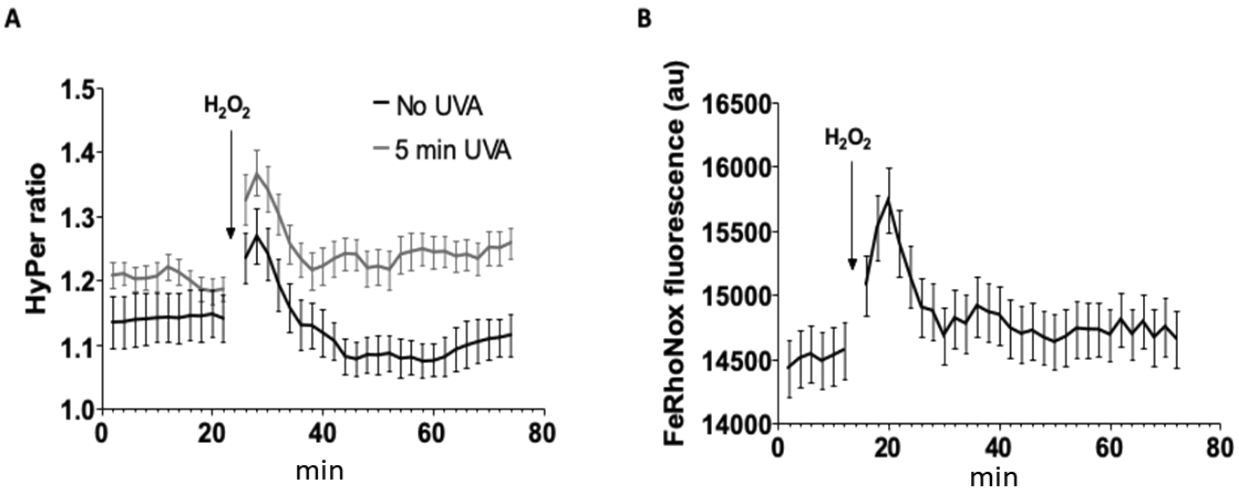

Figure 3. Treatment with exogenous hydrogen peroxide increases labile iron in dermal endothelial cells. (**A**) Dermal endothelial cells (HDBECs), transfected with the HyPer hydrogen peroxide ratiometric fluorescent probe, show an increase in fluorescent signal upon treatment with 100 µM exogenous H_2O_2, regardless of previous UVA irradiation. (**B**) Concurrent increase in labile iron, measured using FeRhoNox fluorescent probe, following exogenous H_2O_2 treatment. Data denote mean ± S.E.M., n=3 replicates.

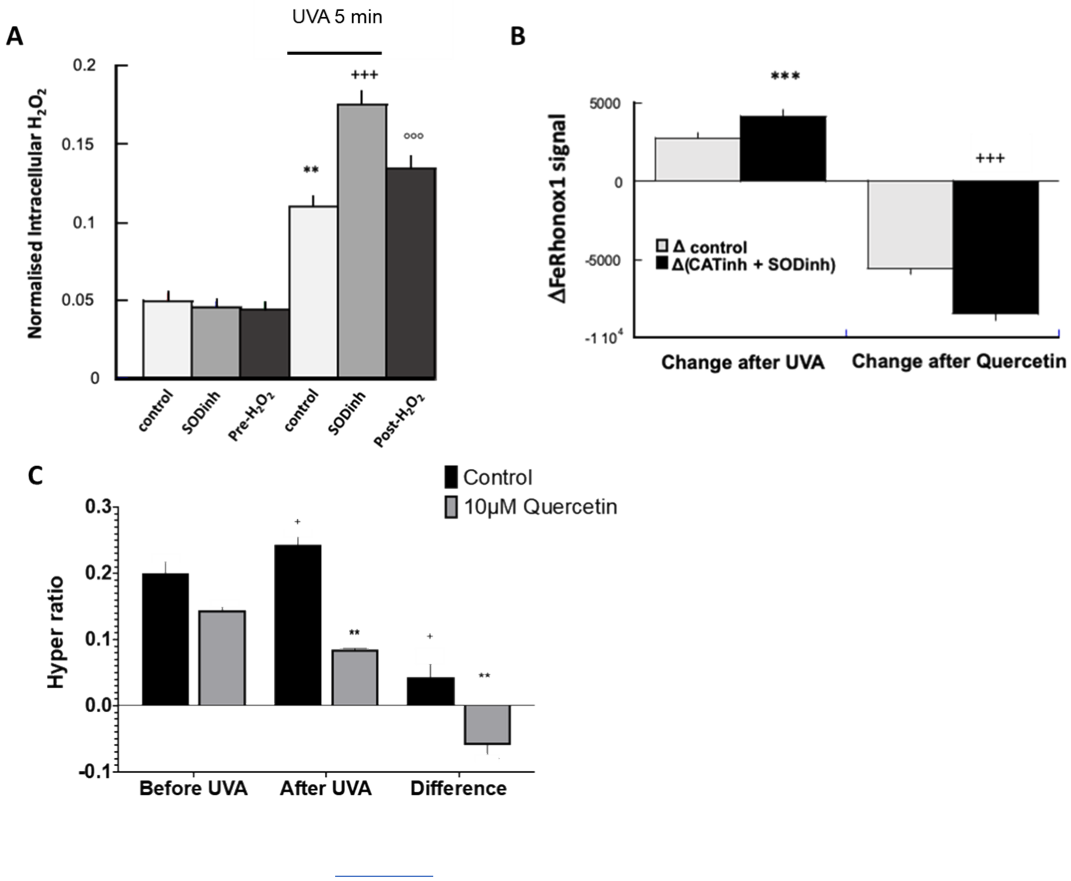

Figure 4. Quercetin inhibits intracellular free iron and hydrogen peroxide in dermal endothelial cells.

(A) HDBECs transfected with HyPer that were pre-treated with SOD inhibitor ATM (4μM)(grey bars) and exposed to UVA for 5 min (≈4 kJ/m^2) show an increase in HyPer signal above control after UVA. Control after UV versus before UVA **P<0.01; SOD inhibitor after UV versus SOD inhibitor, before UVA (+++ P<0.001) Black bars show the effects of exposure of the cell cultures to H_2O_2 (50 μM) on the Hyper signal after versus before H_2O_2 °°° P<0.001.

(B) Change in FeRhoNox signal in HDBECs treated with vehicle (controlor SOD inhibitor ATM (4μM) + 2mM Catalase inhibitor (CATinh) (3-ATZ) after UVA irradiation (***P<0.001). After addition of quercetin (10μM) ($^{+++}$ P<0.001). Thus, quercetin has a significantly greater effect on cells treated with both SOD and catalase inhibitors than controls indicating a higher level of labile Fe(II) prior to quercetin treatment in cells treated with antioxidant inhibitors.

(C) Change in HyPer signal in HDBECs treated with quercetin (10μM) and irradiated with UVA for 5 min (≈4 kJ/m^2). Data denote mean ± S.E.M., n=3 independent cultures, + P < 0.05 difference between before and after UVA (control); **P<0.01, difference between before and after UVA (quercetin) ;

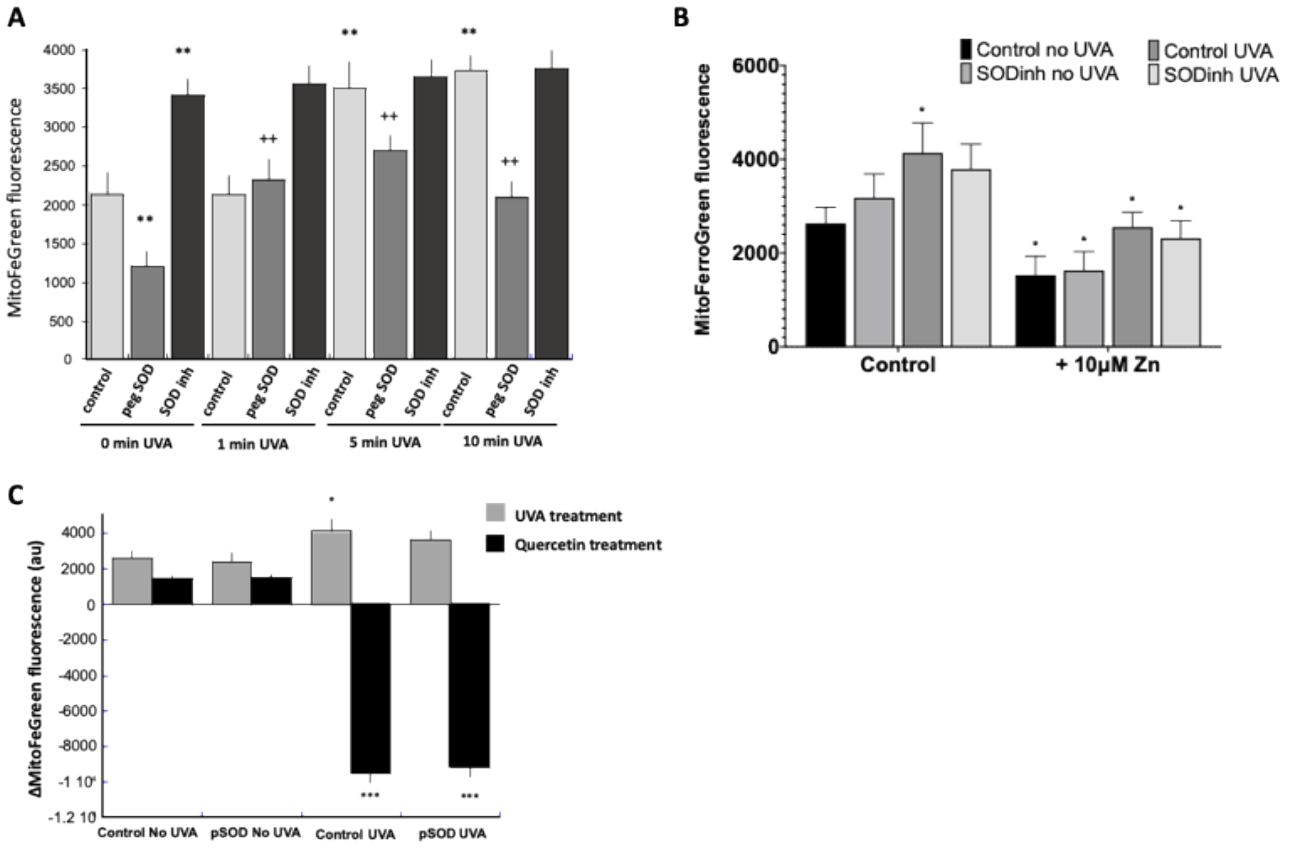

Figure 5. Mitochondrial iron levels change in parallel to cytosolic iron levels in dermal fibroblasts.

(**A**) NHDFs were treated with SOD inhibitor ATM (4µM) or pegSOD (500U/ml), exposed to UVA for 1 -10 min (≈0.8-8 kJ/m^2) and labile iron in the mitochondria measured using MitoFerroGreen fluorescent probe and expressed as relative fluorescence (arbitrary units) ** P < 0.01 column condition versus control (no UVA column 1). ++ P < 0.01, column condition versus SOD inhibition, (no UVA, column 2).

(**B**) NHDFs were treated with SOD inhibitor ATM (4µM) and $ZnCl_2$ (10µM) before being exposed to UVA (≈4 kJ/m^2) and labile iron in the mitochondria measured using MitoFerroGreen fluorescent probe. Condition versus control no UV (column 1) *P<0.05.

(**C**) Change in MitoFerroGreen signal in HDBECs pre-treated with pegSOD (500U/ml) before treatment ± quercetin (10µM) and irradiated with UVA for 5 min (≈4 kJ/m^2)., *P<0.05, Condition relative to control no UVA column 1 ***P<0.001 Condition with quercetin and UVA relative to beforeUVA irradiation. .Data denote mean ± S.E.M., n=3 independent cultures .

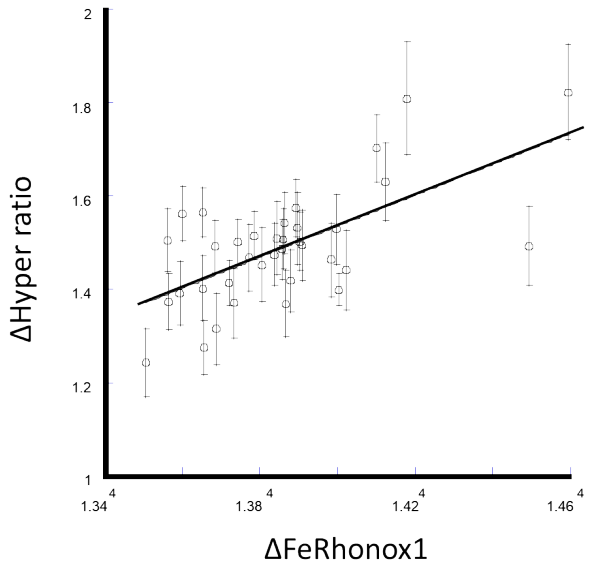

Supplementary Figure S1A. Correlation between the changes in intracellular Fe(II) reported by FeRhonox1 (x axis) and H_2O_2 reported by HyPer signals (y axis) following addition of quercetin (10 **µ**M) to dermal endothelial cells incubated with the SOD inhibitor ATM (4 **µ**M). Data denote means ± S.E.M of Hyper signals, Pearson's correlation coefficient of the best fit linear correlation fit is=0.64 (d.f. 28, $p < 0.001$).

Supplementary Figure S1B

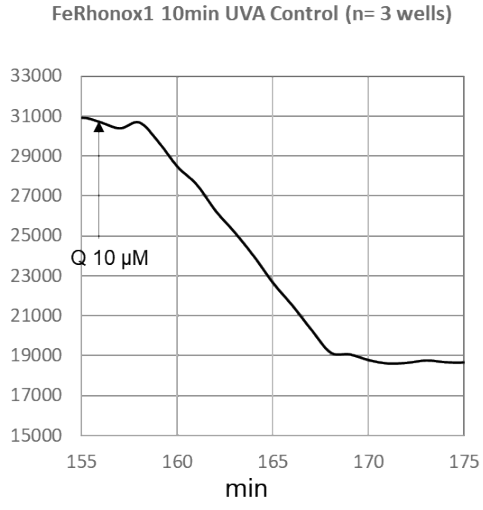

Supplementary Figure S1C

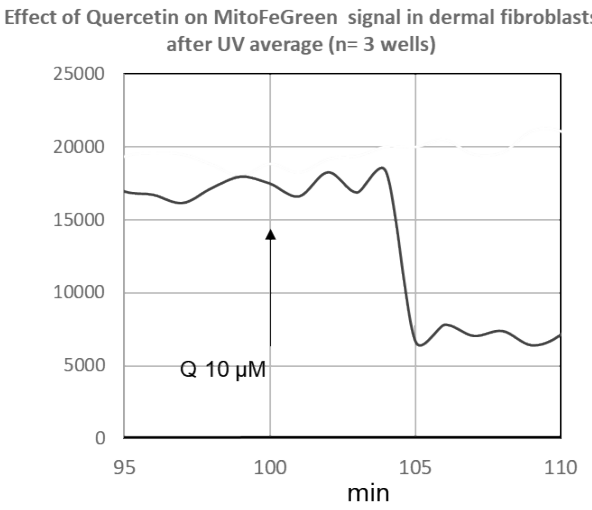

Supplementary Figures S1B and S1C. Output signals showing the time courses of effects of quercetin (10 µM) addition to cell cultures post UVA exposure on FeRhonox1 and MitoFeGreen fluorescence. Figure S1B shows a more gradual and smaller percentage decrease in cytosolic Fe(II) than observed with mitochondrial Fe(II) as reported by MitoFeGreen in Figure S1C.

S1B Quercetin reduces cell FeRhonox1 signal after UVA 10 min by 40% $t_{1/2}$ ≈ 7 min. Quercetin reduces MitoFeGreen signal after UVA 10 min by 65% $t_{1/2}$ ≈ 3 min. No effect of UVA without UVA.

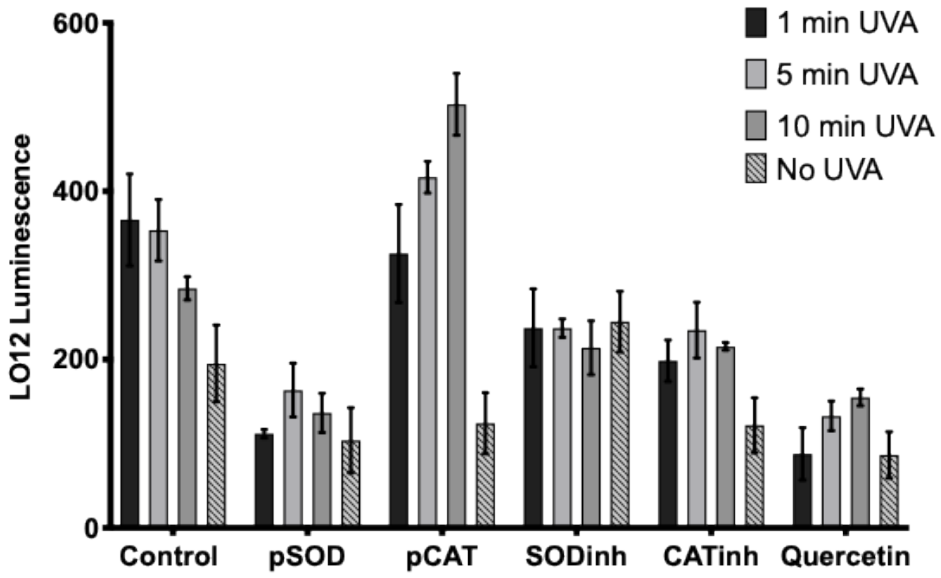

Supplementary Figure S2. Reactive oxygen species detected by L012 are induced by UVA, increased by catalase and reduced by iron chelation with quercetin. NHDFs were treated with pegSOD (500U/ml), SOD inhibitor ATM (4µM), catalase inhibitor 3-AT (2mM) and Quercetin (10µM) with UVA irradiation of 1-10 min (≈0.8-8 kJ/m^2). Mean luminescence signal of intracellular reactive oxygen species was measured using the chemiluminescent probe L012. Catalase increases this signal, ($P < 0.01$), whilst quercetin reduces the signal. Data denote mean ± S.E.M. ($P < 0.001$), n=3-5 replicates.

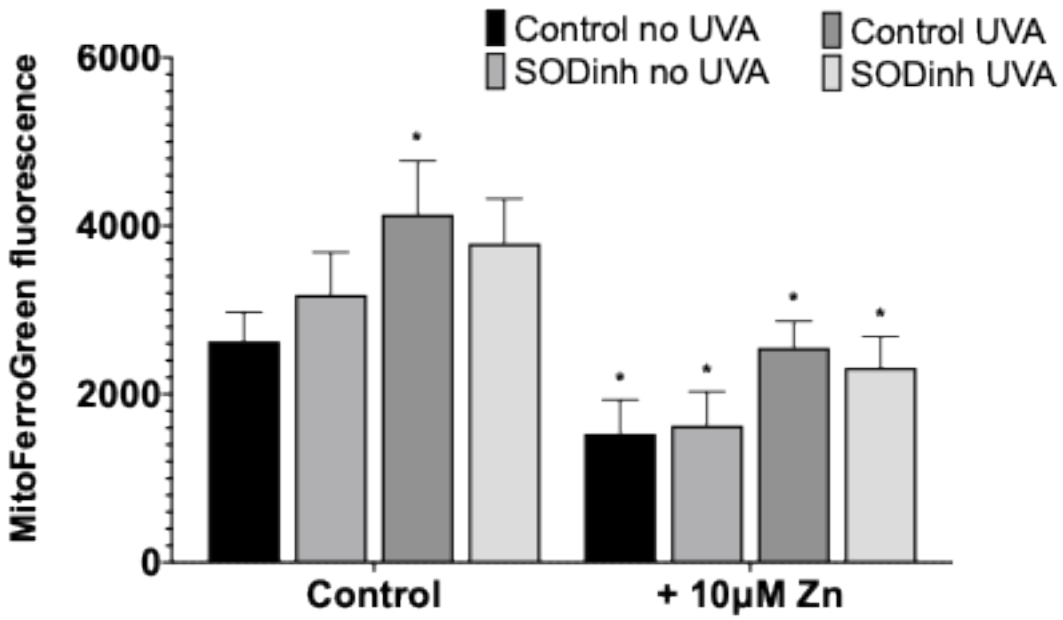

Supplementary Figure S3. Zinc inhibits changes in mitochondrial iron levels following UVA irradiation of dermal fibroblasts. NHDFs were treated with vehicle (DMSO) (Control) or SOD inhibitor ATM (4uM), with or without Zinc (10µM) and exposed to UVA for 10 min (≈8 kJ/m^2) and labile iron in the mitochondria measured using MitoFerroGreen fluorescent probe. Data denote mean ± S.E.M., n=3 independent cultures, P<0.05.